Materials Science Forum *Online: 2008-09-09*
ISSN: 1662-9752, Vols. 595-598, pp 483-490
doi:10.4028/www.scientific.net/MSF.595-598.483

Electrochemical study of the corrosion of metals in molten fluorides

Stéphanie Fabre[1,a], Céline Cabet[2,b], Laurent Cassayre[3,c], Pierre Chamelot[3,d]
Jörgen Finne[1,e], Didier Noël[1,f], Pierre Taxil[3,g]

[1]EDF R&D – Département Matériaux et Mécanique des Composants - Groupe Chimie et Corrosion - 77818 Moret-sur-Loing Cedex - France

[2]CEA Saclay - DEN/DANS/DPC/SCCME – 91191 Gif-sur-Yvette – France

[3]LGC – UMR 5503 - Université Paul Sabatier – 31062 Toulouse Cedex 9 - France[a]stephanie-externe.fabre@edf.fr, [b]celine.cabet@cea.fr, [c]cassayre@chimie.ups-tlse.fr, [d]chamelot@chimie.ups-tlse.fr, [e]jorgen.finne@edf.fr, [f]didier.noel@edf.fr, [g]taxil@chimie.ups-tlse.fr,

Keywords: Molten salts, fluorides, nickel alloys, electrochemistry.

Abstract. Resistance to corrosion of the structural materials is a key factor for nuclear applications that use molten fluorides. Low chromium, nickel-base alloys are regarded as the most suitable metallic materials. In a first approach, corrosion of some pure metallic constituents Ni, Mo, W and Fe, was studied by electrochemical techniques. Linear voltammetry was applied in LiF-NaF and LiF-AlF_3, in the temperature range 900-1100°C.

The relative stability of the metals in LiF-NaF is established. To determine the corrosion current density, three methods are presented, two based on the Tafel extrapolation method and the third one being the polarization resistance method. Results regarding corrosion rates are compared. Two corrosion behaviors are observed: on the one side, Ni, Mo and W and on the other side Fe. The difference might come either from different corrosion mechanisms or from a different number of exchanged electrons. The corrosion rate increases with temperature following the Arrhenius law. However, further experiments are needed in order to identify the key parameters that influence the corrosion in the different melts.

Introduction

Fluoride salts are contemplated for different applications such as heat carrier, electrolyte, solvent for the reprocessing of spent nuclear fuel or fuel in a molten salt reactor. Indeed they show the following characteristics: good stability at high temperatures, resistance to radiations, capacity to dissolve fission products, compatibility with the structural and the moderator materials, low cross section capture of neutrons [1].

The compatibility of the structural materials with the fluoride medium is a key factor for the feasibility of processes which use these molten salts. Metallic materials have especially to resist corrosion by fluoride melts at high temperatures (typically 500-700°C).

Research programs have already been completed in the 50-70's in support of the development of a molten salt reactor. Many types of alloys were tested in mixtures of LiF, BeF_2, NaF, ZrF_4, ThF_4 etc. Nickel-base alloys were proved to be the most resistant to corrosion. A dedicated alloy, under the brand name Hastelloy-N, was developed by ORNL (Oak Ridge National Laboratory-USA) based on its mechanical as well as corrosion properties (in air and fluoride melts). This nickel-base alloy is strengthened by molybdenum (16wt. %), and contains low chromium and iron percentages (7 and 5wt. %).

Tests were carried out in thermal convection and forced-circulation loops. Analysis of salt samples and observation of the corroded alloy specimens evidenced that a mass transfer occurred along the temperature gradient [2] which was influenced by different parameters: material nature, temperature gradient, level of impurities etc [3]. Hastelloy N globally showed a good compatibility with highly purified molten fluorides [4]. However few studies were published regarding the corrosion mechanisms.

The aim of this work is to give an insight on the basis of the corrosion of nickel-base alloys in molten fluoride salts. In a first approach, the corrosion rates of the pure metals, Ni, Mo, W and Fe were estimated in static conditions by electrochemical methods (voltammetry) and the roles of the temperature and of the chemical composition of the melt were investigated.

Experimental

Electrochemical reactor. The experiments were conducted in an electrochemical reactor dedicated to studies of metals in molten fluorides at high temperatures. Fig. 1 presents a scheme of the set-up.

The measurements are carried out at temperatures up to 1200°C using a 3-zone resistance-heated furnace (AET Technology). The cell is made of a graphite jacket within which a glassy carbon crucible containing the salt (200g) is placed. The jacket protects the refractory steel container from the aggressive gasses and vapours. The cell is hermetically sealed by means of a water-cooled lid with an O-ring seal. All works are done under a circulating high purity argon atmosphere. The electrode assemblage is dipped into the melt from the top of the reactor and this electrochemical set-up is connected to an Autolab PGSTAT 10 potentiostat, with GPES software.

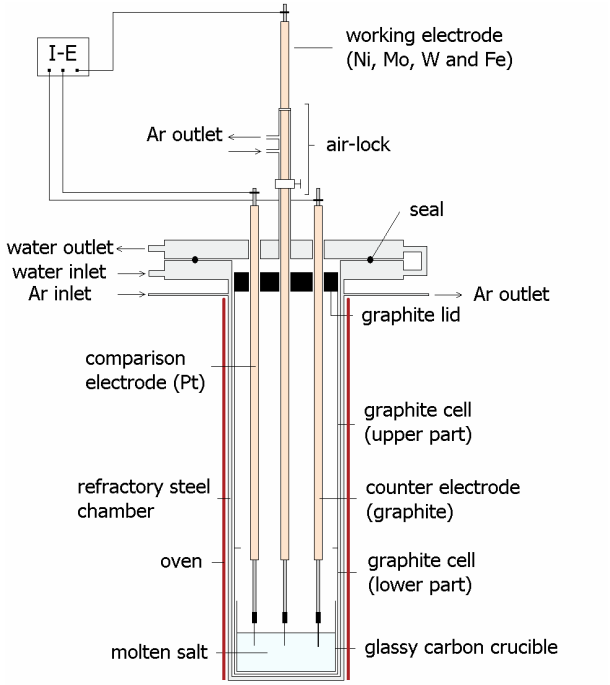

Fig. 1. Schematic of the set-up.

Electrode materials. A three-electrode set-up was used. Working electrodes were made of Ag, Ni, Mo, W and Fe 1mm diameter wires. The metals were purchased from Goodfellow with a purity of at least 99.98%. The immersed length was around 1cm (measurement made at the end of the experiment), corresponding to a surface of the working electrode in-between 0.32 and 0.42cm².

A 3mm diameter vitreous carbon rod purchased from Goodfellow was used as a counter electrode.

The comparison electrode was a 1mm diameter platinum wire with a purity of 99.99% (Goodfellow). A preliminary experiment allowed to determine that the potentials were reproducible for at least 2 weeks. Each electrode was attached to an Inconel 600 conducting rod inserted and bonded into an alumina tube (for electrical insulation).

Molten fluorides. Two different molten salt mixtures were used: LiF-NaF (61/39 mole %) and LiF-AlF_3 (85/15 mole %). These compositions correspond to eutectic points of each binary systems [5] and the liquidus temperatures are 649° and 720°C respectively.

LiF was purchased from Merck, with a 99% minimum purity. NaF and AlF_3 were purchased from Alfa Aesar, with a minimum purity of 99.99%.

Humidity and oxygen are the main impurities of the melt and have to be removed so far as possible. The purification of the salt was achieved with a step-by-step heating procedure under vacuum. The mixture was finally melted under an argon atmosphere. The purity of the melt was checked after the melting by cyclic voltammetry (100mV/s) on a silver electrode. The absence of any other redox system than those of the oxidation of Ag and of the formation of the AgLi alloy in the cathodic region validated the purity level. It is assumed that the quantity of impurities (H_2O and O_2) in the melt is below 5ppm and is quite stable.

Electrochemical methods. Experimental measures are done by electrochemical methods in order to indentify the mechanisms controlling corrosion. The Tafel and polarization resistance techniques can be applied in molten fluorides to measure corrosion rates as, commonly, no oxide scale forms [6]. Linear voltammetry was used with a sweep rate of 1 to 10mV/s. Experiments at different sweep rates showed that 1mV/s was the most adapted sweep rate to study the metals and enabled to be at quasi-equilibrium. For each metal, two sets of data were executed at 1mV/s to apply the Tafel method (recording of the variations of I as a function of E from the corrosion potential towards anodic potentials and then from the corrosion potential towards cathodic potentials) and the resistance polarization method (recording of the variations of I as a function of E from the corrosion potential to E_{corr}+40mV and then to E_{corr}-40mV – other ΔE were tested and $I=f(E)$ was still linear for ±40mV hence the choice) [7].

Tafel method. The Tafel method was used to determine the value of the corrosion current density and the Tafel coefficients to be used in the resistance polarization method. The variation of the logarithm of the current density was plotted as a function of the overpotential using the data obtained from the linear voltammetry at 1mV/s. The linear portion of the curves close to a null overpotential could be extrapolated using the Tafel method, with Eq. 1 and Eq. 2 respectively in the anodic and cathodic parts [8]:

$$\ln(i) = \frac{\alpha_{ox} nF}{RT}\eta + \ln|i_{corr}| = \frac{1}{\beta_{ox}}\eta + \ln|i_{corr}|. \quad (1)$$

$$\ln(i) = -\frac{\alpha_{red} nF}{RT}\eta + \ln|i_{corr}| = -\frac{1}{\beta_{red}}\eta + \ln|i_{corr}|. \quad (2)$$

Where i=current density (A/cm²), α_{ox} and α_{red}=anodic and cathodic charge transfer coefficients, n=number of exchanged electrons, F= Faraday's constant (C/mol), R=ideal gas constant (J/mol.K), T=temperature (K), η=overpotential (V), i_{corr}=corrosion current density (A/cm²) and β_{ox} and β_{red}=anodic and cathodic Tafel coefficients.

Polarization resistance method. The Stern and Geary equation (Eq. 3) established the relationship between the corrosion current density and the polarization resistance R_p defined as $(\partial E/\partial i)_{\eta=0}$ [9]. The linear voltammetry curves with a sweep rate of 1mV/s within 40mV of the corrosion potential showed a linear region from which R_p could be calculated. The ohmic drop was not corrected as measurements showed that the value of the resistance was negligible compared to the R_p values.

$$i_{corr} = \frac{1}{2.3R_p}\frac{\beta_{ox}\beta_{red}}{\beta_{ox}+\beta_{red}}. \quad (3)$$

Where R_p=polarization resistance (Ω.cm²).

The corrosion rate given by Eq. 4 is obtained from the corrosion current density value:

$$v_{corr} = 3.15\times10^{11}\frac{i_{corr}M}{\mu nF}. \quad (4)$$

Where v_{corr}= corrosion rate (mm/year), M=atomic weight (g/mol) and μ=density (kg/m^3).

Results and Discussion

Thermochemical calculations. Potential-oxoacidity diagrams were established with the pure components database from the HSC software [10]. The stability domains of the metallic species are represented as a function of the potential vs. $F^-/F_2(g)$ (Y axis) and of the co logarithm of the activity of the most stable oxide of the melt, *pa(oxide)=-log[oxide]* (X axis).

In the case of LiF-NaF, the oxide is Li_2O. The equilibriums were calculated using the Nernst's equation [11] with the following assumptions: $F^-/F_2(g)$ was the reference system for potentials, the activities of the solutes were taken equal to 1 and the activity of the salt components was their molar ratio (a(LiF)=0.6 and a(NaF)=0.4).

Fig. 2 presents the diagrams of Ni and Fe in LiF-NaF at 1100K. The lower limit corresponds to the reduction of the solvent (NaF) and the upper limit is the oxidation of O^{2-} ions.

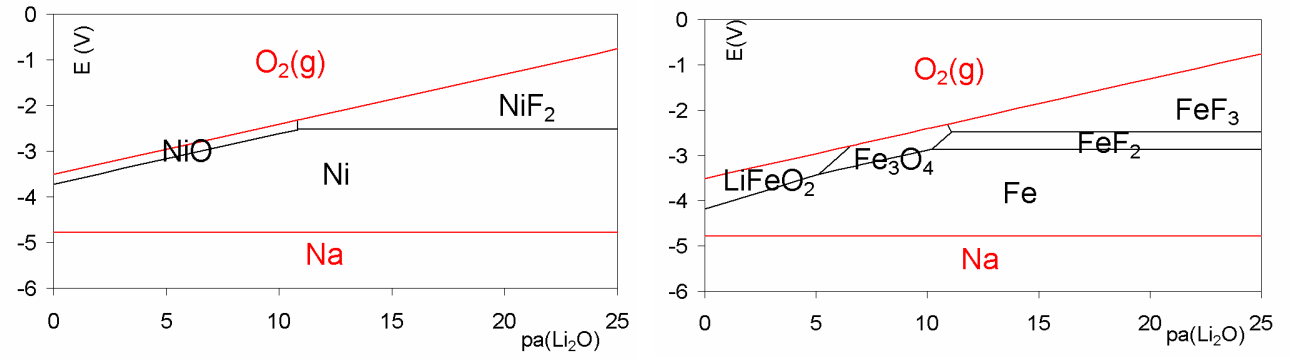

Fig. 2. Potential-oxoacidity diagrams of Ni and Fe in LiF-NaF at 1100K.

Those diagrams enable to get a global idea of the chemistry of the melt in given conditions. Because of the assumptions made (activity=1), it is difficult to use those diagrams as an exact representation

of the domains of existence of the different species of a metal as a function of $pa(Li_2O)$ (whose value during the experiment is unknown).

Corrosion behaviour of the metals. The pure metals, Ni, Mo, W and Fe, were studied in LiF-NaF at 900°C. Fig. 3 presents the linear voltammograms of those metals. In the cathodic region the reaction is similar for all four metals: reduction of the solvent. As the linear voltammograms superimposed quite well in this domain, the anodic parts of the voltammograms of each metal can be compared. The sharp increase in the anodic region corresponds to the anodic dissolution of the metals. Based on their oxidation potentials, the materials can be classified in order of stability as follows: Fe < Ni < Mo < W. Fe corrodes at the lowest potential, then Ni and Mo, while W is the most stable metal.

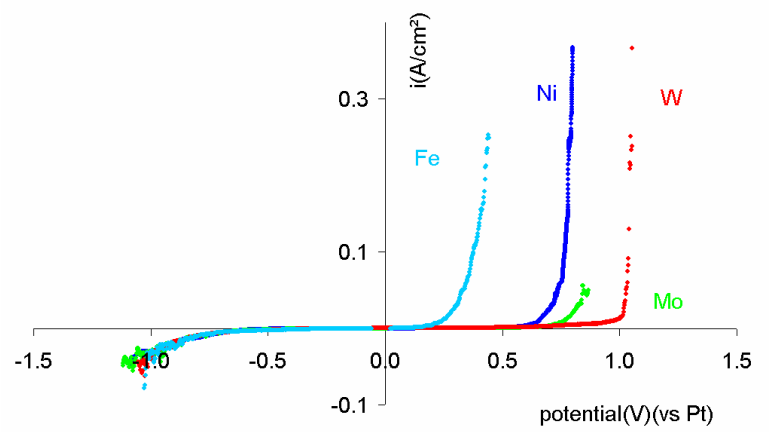

Fig. 3. Linear voltammetry of Fe, Ni, Mo and W in LiF-NaF at 900°C (sweep rate: 1mV/s, potential scanning from free potential towards anodic potentials and then from free potential towards cathodic potentials).

Fig. 4 (a) presents linear voltammetry for the four metals in LiF-NaF at 900°C.

The logarithm of the current density is plotted as a function of the overpotential. This Tafel representation evidences two different behaviours towards corrosion in the anodic part: Ni, Mo and W show similar linear evolutions, whereas the voltammogram of Fe has a steeper slope. Therefore two hypotheses can be formulated with respect to Eq.1: either the metals have different corrosion mechanisms (different values of the transfer coefficient, α) or they have a different number of exchange electrons.

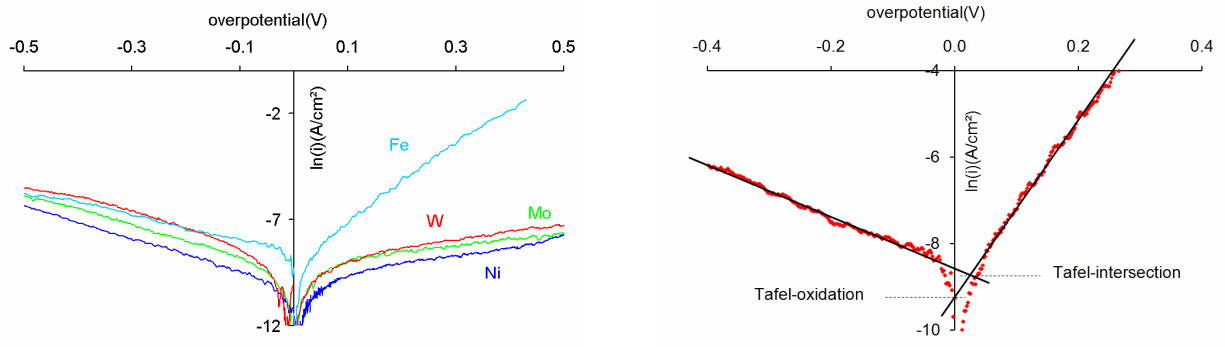

a) b)

Fig. 4. Tafel representation of the linear voltammetry of a) Ni, Mo, W and Fe in LiF-NaF at 900°C, b) Fe in LiF-NaF at 900°C (sweep rate: 1mV/s, potential scanning from free potential towards anodic potentials and then from free potential towards cathodic potentials).

Table.1 reports the Tafel coefficients, β_{ox} and β_{red}, the corrosion current densities from R_p and from two interpretations of the Tafel method (Tafel-oxidation being the calculation of i_{corr} using only the anodic equation and Tafel-intersection being the calculation of i_{corr} from the intersection of the anodic and cathodic equations as shown in Fig. 4 b)) and the corrosion rates from Eq. 4. In order to calculate the corrosion rates, the number of exchanged electrons needs to be known. The following assumptions were made based on thermochemical data (most stable species for each metal in LiF-NaF): for Ni, Mo and Fe, $n=2$ and for W, $n=4$.

For a same metal, the values of i_{corr} and v_{corr} depend on the method used to make the calculations. As shown in Fig. 4 b), the two points taken for $ln(i_{corr})$ can be somewhat shifted due to the Tafel extrapolation. The difference is small but noticeable for Fe and negligible for Ni, Mo and W. The Tafel methods and the polarization resistance method are interpretation of two different sets of data hence the discrepancy between the methods. Further calculations indicated that the resistance polarization method showed a good agreement between experimental results and theory with respect to the Arrhenius law (Eq. 5). The values of v_{corr} enable to classify the metals towards their resistance to corrosion (based on the R_p results): Ni, W < Fe < Mo. Mo being the metal that corrodes the fastest.

It is worth noticing that Fig. 4 shows no occurrence of any pseudo-passivity. So the corrosion corresponds to the pure dissolution of the metals, either directly or with the formation of an intermediate compound.

The comparison of the anodic Tafel coefficients verifies the direct observation of the curves in Fig. 4: Ni, Mo and W may follow a similar corrosion mechanism or have the same number of exchanged electrons whereas Fe behaves differently.

Table.1 Results for Ni, Mo, W and Fe in LiF-NaF at 900°C (no precision is indicated for the values of β because the error is inferior to 5.10^{-3}).

Metal	β_{ox}	β_{red}	Corrosion rate	Tafel-oxidation i_{corr} [A/cm²] v_{corr} [mm/year]	Tafel-intersection i_{corr} [A/cm²] v_{corr} [mm/year]	R_p i_{corr} [A/cm²] v_{corr} [mm/year]
Ni	0.27	0.12	i_{corr}	$(4.6 \pm 0.2)\ 10^{-5}$	$(4.2 \pm 0.3)\ 10^{-5}$	$(4.0 \pm 0.4)\ 10^{-5}$
			v_{corr}	0.5 ± 0.01	0.45 ± 0.03	0.43 ± 0.04
W	0.25	0.13	i_{corr}	$(1.1 \pm 0.1)\ 10^{-4}$	$(1.1 \pm 0.1)\ 10^{-4}$	$(4.5 \pm 0.6)\ 10^{-5}$
			v_{corr}	0.82 ± 0.01	0.89 ± 0.07	0.43 ± 0.04
Mo	0.29	0.15	i_{corr}	$(9.6 \pm 0.04)\ 10^{-5}$	$(9.3 \pm 0.6)\ 10^{-5}$	$(6.7 \pm 0.6)\ 10^{-5}$
			v_{corr}	1.46 ± 0.01	1.42 ± 0.09	1.05 ± 0.09
Fe	0.05	0.16	i_{corr}	$(1.2 \pm 0.1)\ 10^{-4}$	$(1.7 \pm 0.2)\ 10^{-4}$	$(7.0 \pm 0.7)\ 10^{-5}$
			v_{corr}	1.41 ± 0.01	1.91 ± 0.22	0.81 ± 0.08

Influence of temperature. The metals were tested in LiF-NaF at three temperatures: 900, 1000 and 1100°C. Values of i_{corr} were obtained following the method described above (coupling Tafel coefficients and R_p measurements). Fig. 5 presents the evolution of $ln(i_{corr})$ with the inverse of the temperature: the curves $ln(i_{corr})$ as a function of $(-1/T)$ show a linear variation. Table.2 presents the corrosion rates at each temperature according to Eq. 4 and the values of the activation energy E_a calculated from Fig. 5 and Eq. 5:

$$i_{corr} = i^{\circ} \exp\left(\frac{-E_a}{RT}\right). \quad (5)$$

Where $i°$=pre-factor (A/cm²), E_a=activation energy (J/mol), R=ideal gas constant (J/mol.K) and T=temperature (K).

For each metal, the corrosion rate increases with temperature. The more important the value of the activation energy is, the more the corrosion rate increases between two temperatures. It is possible to classify the metal towards their sensitivity to temperature by comparing the values of the activation energies: Ni < Mo < W < Fe. At this state of the study, those values of activation energies cannot be related to any particular mechanism.

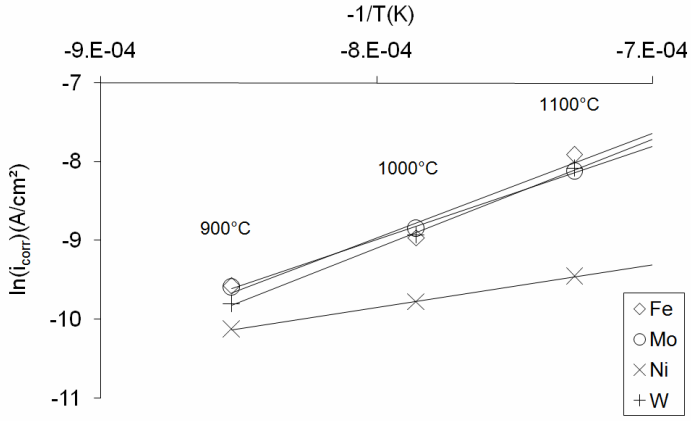

Fig. 5. Influence of temperature on corrosion of Ni, Mo, W and Fe in LiF-NaF (precision is ±0.1A/cm²).

Table.2 Values of the corrosion rates at 3 temperatures and of the activation energies of Ni, Mo, W and Fe in LiF-NaF.

Metal	v_{corr} [mm/year]			E_a [kJ/mol]
	900°C	1000°C	1100°C	
Ni	0.43 ± 0.04	0.62 ± 0.05	0.85 ± 0.07	42.29 ± 0.04
W	0.43 ± 0.04	1.04 ± 0.09	2.41 ± 0.2	114.85 ± 0.64
Fe	0.81 ± 0.08	1.49 ± 0.13	4.28 ± 0.46	110.45 ± 2.49
Mo	1.05 ± 0.09	2.2 ± 0.2	4.56 ± 0.46	99.14 ± 3.60

Influence of the composition of the melt. The metals were characterised in another salt mixture, LiF-AlF_3. Table.3 reports the corrosion current densities and the corresponding corrosion rates. The values for LiF-NaF were calculated with the methods previously presented, but for LiF-AlF_3, the values of i_{corr} were estimated by a pure Tafel method (intersection of the extrapolated linear part of the $ln(i)=f(\eta)$ curve with the $ln(i)$ axis).

Table.3 Corrosion current density and corrosion rate of Ni, Mo, W and Fe in two LiF-based salts at 900°C (results calculated with R_p for LiF-NaF and Tafel-oxidation for LiF-AlF_3).

Metal	i_{corr} [A/cm²]		v_{corr} [mm/year]	
	LiF-NaF	LiF-AlF_3	LiF-NaF	LiF-AlF_3
Ni	(4.0 ± 0.4) 10^{-5}	(9.3 ± 0.4) 10^{-3}	0.43 ± 0.04	99.7 ± 0.1
W	(4.5 ± 0.6) 10^{-5}	(4.2 ± 0.1) 10^{-2}	0.43 ± 0.04	325.6 ± 0.1
Mo	(6.7 ± 0.6) 10^{-5}	(5.1 ± 0.2) 10^{-3}	1.05 ± 0.09	77.4 ± 0.1
Fe	(7.0 ± 0.7) 10^{-5}	x	0.81 ± 0.08	x

For a given metal, the corrosion rate appears to increase as follows: LiF-NaF < LiF-AlF_3. Several hypotheses may be suggested in order to explain this observation. It may be assumed that the mixtures have different fluoroacidities (solvating capability of F^- ions) and oxoacidities. For the last named parameter there is a general lack of data and complementary experiments are needed in order to determine free oxide concentration and evaluate its impacts on corrosion rates.

However, concerning fluoroacidity, LiF-AlF_3 is more fluoroacid than LiF-NaF and it can be observed that the corrosion of the metal increases with the fluoroacidity of the melt, which is in good agreement with what is generally assumed.

Conclusion

Electrochemical methods allowed studying the corrosion behaviour of some pure metallic elements of the nickel base alloys that are of interest for nuclear applications using molten fluorides. Validation of the experimental tools and procedures was based on the high purification levels that were achieved and on the good repeatability of the results. Stability order of the metals was established according to their respective oxidation peaks in LiF-NaF at 900°C. Linear voltammograms evidenced two corrosion behaviours: on the one side Ni, Mo and W and on the other side Fe. The difference could be due to different corrosion mechanisms or a different number of exchanged electrons. In any case, passivation has never occurred in the given test conditions (very low oxide content). Pure Tafel methods showed to be less sensitive than the method based on the coupling of the Tafel representation and the determination of the polarisation resistance to assess i_{corr}. In LiF-NaF at 900°C, nickel and tungsten corrode the less, while molybdenum is the easiest to corrode. The corrosion rate increases with temperature following the Arrhenius law. However, further experiments in LiF-NaF, LiF-AlF_3 and in a third fluoride mixture, LiF-CaF_2, are needed in order to identify the key parameters that influence the corrosion in these melts. Moreover, binary nickel alloys will be evaluated according to the same methods as the pure metals and the influence of oxides in the melts on the corrosion behaviour of the metals will be studied.

References

[1] W. R. Grimes, et al., in: Molten-Salt Reactor Program, ORNL-4812, 5. Fuel and coolant chemistry (1972), p.95.

[2] J. A. Lane, et al., in: Fluid Fuel Reactor, edited by Addison-Wesley, volume Part II of chapter 13, (1958).

[3] J. W. Koger: Corrosion Vol. 30 (1974), p.125.

[4] J. W. Koger, in: Molten-Salt Reactor Program, ORNL-4832, 12.3. Salt Corrosion Studies (1972), p.124.

[5] J. Sangster and A. D. Pelton: J. Phase Equilib. Vol. 12 (1991), p.511.

[6] V. M. Azhazha, et al.: Problems of Atomic Science and Technology Vol. 4 (2005),

[7] D. Landolt, in: Corrosion et chimie de surfaces des métaux, edited by Presses polytechniques et universitaires romandes, volume 12 of Traité des matériaux, chapter 4, Alden Press (1993).

[8] A. J. Bard and L. R. Faulkner, in: Electrochimie - Principes, méthodes et applications, edited by Masson, volume of chapter 3, (1983).

[9] R. Scully: Corrosion Vol. 56 (2000), p.199.

[10] HSC Chemistry, v.5.1, Outokumpu Research Oy (2002).

[11] A. J. Bard and L. R. Faulkner, in: Electrochimie - Principes, méthodes et applications, edited by Masson, volume of chapter 2, (1983).